SOCIETY FOR EXPERIMENTAL BIOLOGY

Journal of Experimental Botany
https://doi.org/10.1093/jxb/erad227 Advance Access Publication 23 June 2023

RESEARCH PAPER

Axial conduit widening, tree height, and height growth rate set the hydraulic transition of sapwood into heartwood

Giai Petit[1,*], Maurizio Mencuccini[2,3], Marco Carrer[1], Angela Luisa Prendin[1,4] and Teemu Hölttä[5]

[1] Università degli Studi di Padova, Dept. TeSAF, Viale dell'Università 16, 35020 Legnaro (PD), Italy
[2] CREAF, Bellaterra (Cerdanyola del Vallès), E08193, Spain
[3] ICREA, Pg. Lluís Companys 23, Barcelona, 08010, Spain
[4] Department of Biology, Ecoinformatics and Biodiversity, Aarhus University, Ny Munkegade 114-116, building 1540, 8000 Aarhus C, Denmark University of Aarhus, Denmark
[5] Institute for Atmospheric and Earth System Research/ Forest Sciences, Faculty of Agriculture and Forestry, University of Helsinki, Latokartanonkaari 7, FI 00014 Helsinki, Finland

[*] Correspondence: giai.petit@unipd.it

Received 31 January 2023; Editorial decision 7 June 2023; Accepted 12 June 2023

Editor: Anja Geitmann, McGill University, Canada

Abstract

The size-related xylem adjustments required to maintain a constant leaf-specific sapwood conductance (K_{LEAF}) with increasing height (*H*) are still under discussion. Alternative hypotheses are that: (i) the conduit hydraulic diameter (*Dh*) at any position in the stem and/or (ii) the number of sapwood rings at stem base (*NSWr*) increase with *H*. In addition, (iii) reduced stem elongation (Δ*H*) increases the tip-to-base conductance through inner xylem rings, thus possibly the *NSWr* contributing to K_{LEAF}. A detailed stem analysis showed that *Dh* increased with the distance from the ring apex (*DCA*) in all rings of a *Picea abies* and a *Fagus sylvatica* tree. Net of *DCA* effect, *Dh* did not increase with *H*. Using sapwood traits from a global dataset, *NSWr* increased with *H*, decreased with Δ*H*, and the mean sapwood ring width (*SWrw*) increased with Δ*H*. A numerical model based on anatomical patterns predicted the effects of *H* and Δ*H* on the conductance of inner xylem rings. Our results suggest that the sapwood/heartwood transition depends on both *H* and Δ*H*, and is set when the carbon allocation to maintenance respiration of living cells in inner sapwood rings produces a lower gain in total conductance than investing the same carbon in new vascular conduits.

Keywords: Allometry, carbon allocation, conduit widening, heartwood, hydraulic conductance, hydraulic model, sapflow, sapwood, tree growth, water relations.

Introduction

In mature trees, the xylem tissues accumulated by secondary growth (i.e. xylem layers or rings, visually recognizable in species with seasonal dormancy of cambial activity) account for the majority of the total plant biomass and for nearly the entire length of the root-to-leaf hydraulic path. The pivotal physiological functions performed by the xylem are water and nutrient transport through its vascular elements, mechanical support, and the different metabolic activities carried out by its living cells. During ontogeny, trees have to cope with the negative effects of being taller on the efficiency of water

transport and on the carbon allocation required for the build-up and maintenance of a continuously larger xylem biomass (Mencuccini *et al.*, 2007; Givnish *et al.*, 2014). However, only an outer set of xylem layers (i.e. rings) of the entire three-dimensional (3D) xylem architecture remains alive and functional for water transport (i.e. the sapwood).

The transition of sapwood into non-functional and non-living xylem (i.e. the heartwood) has been extensively investigated. The sapwood turnover rate (i.e. the number of years required to turn a sapwood ring into heartwood) is relatively constant along the trunk and across individuals (Sellin, 1994). Accordingly, xylem ageing has been commonly hypothesized as the main driver for heartwood formation (Wilkes, 1991; Spicer, 2005; Spicer and Holbrook, 2007). However, the sapwood turnover rate is variable both across species (e.g. from very few sapwood rings in ring-porous species to >100 in some conifers: Spicer, 2005) and at the intraspecific level across environmental settings (e.g. fast versus slow growing trees: Sousa *et al.*, 2013). Radially from outer to inner sapwood, the water flow rate typically decreases (Phillips *et al.*, 1996; Jiménez *et al.*, 2000; Gartner and Meinzer, 2005; Zhao *et al.*, 2018). At the sapwood/heartwood transition, it becomes negligible (James *et al.*, 2002; Spicer, 2005; Beauchamp *et al.*, 2013), and the metabolic rate of living xylem cells substantially decreases (Bamber, 1976; Spicer, 2005).

A better knowledge on sapwood functionality and therefore its transition into non-functional heartwood would require a much better understanding of how the inner sapwood rings are connected to the (in many cases much) younger foliage (Maton and Gartner, 2005). For instance, according to staining experiments, the original xylem vasculature connected to needles remain functional for several years in some conifer species (Maton and Gartner, 2005). Instead, foliage of the upper and lower crown has been reported to be better supplied by outer and inner sapwood, respectively (Fiora and Cescatti, 2008). However, despite the recognition of axial and radial patterns of xylem-specific conductivity (Spicer and Gartner, 2001), the potential effects of the anatomical characteristics of the whole xylem architecture on the hydraulic efficiency of the different sapwood rings has never been investigated.

The tree xylem architecture can be described as a series of conical layers, the new ones superimposed on top of the older ones as the tree increases in height and diameter. The typical radial and axial anatomical patterns of xylem conduit diameter at the individual level in mature trees are well known since the observations of Sanio (1872): the diameter of xylem conduits progressively increases radially with the ring's cambial age from pith outwards until a maximum diameter is reached and maintained until the bark (Sanio's first law); the maximum diameter in the outermost rings decreases from the stem base towards the apex (i.e. it tapers). The long-standing view that conduit size depends on cambial age (Schulte, 2012) has been recently challenged by the evidence that in the newly formed (i.e. outermost) xylem layer the vascular conduits progressively increase in lumen diameter (D) because of the longer time required for cell enlargement in conduits at increasing distance from the stem apex (DFA) (Anfodillo *et al.*, 2012), and that this widening pattern is well approximated by a power function:

$$D = a \times DFA^{b} \quad (1)$$

with a being the allometric constant and b the scaling exponent. a is certainly dependent on the xylem anatomy of the different species (e.g. conifer tracheids and vessels of ring-porous or diffuse-porous species) (Anfodillo *et al.*, 2013), but is also reported to vary between trees of different sizes (Olson *et al.*, 2014; Prendin *et al.*, 2018a; Echeverría *et al.*, 2019) and subjected to different environmental conditions (Petit *et al.*, 2016; Kiorapostolou and Petit, 2019; Kiorapostolou *et al.*, 2020). Instead, the limited variability of b (between 0.1 and 0.4) reported in the literature for many species of different sizes (Anfodillo *et al.*, 2013; Koçillari *et al.*, 2021) would suggest a strong conservativism of this parameter also during ontogeny. However, only a few studies have tested this hypothesis at the single-tree level (Weitz *et al.*, 2006; Prendin *et al.*, 2018b). The conservativism of b during ontogeny would also imply that the diameter of xylem conduits increases radially from pith to bark because of the increase in stem length with ontogeny, and thus is not causally related to cambial age (Carrer *et al.*, 2015).

If the anatomical characteristics of each xylem ring are DFA dependent, it follows that the sapwood-specific hydraulic conductivity is not homogeneous axially and radially (Pothier *et al.*, 1989).

Since the hydraulic conductance of xylem conduits [conifer tracheids and angiosperm vessels scale inversely to their length and directly to the fourth power of their diameter (Hagen–Poiseuille law: Tyree and Ewers, 1991)], two important hydraulic properties of the xylem transport system are related to b. First, the basipetal increase in conduit lumen diameter from the stem apex to the base can effectively reduce, but not eliminate, the negative effect of path length on the total path conductance (hereafter called the H effect), and such a compensatory effect is stronger for high b values (Becker *et al.*, 2000; Petit and Anfodillo, 2009). Secondly, the hydraulic conductance of the same xylem file in the topmost stem internode (i.e. the annual stem elongation, ΔH) is inversely proportional to its length (hereafter called the ΔH effect) by a factor that decreases with b (i.e. other things being equal, the conductance of the apical shoot in a tree with high ΔH is lower than that of a tree with low ΔH, with the difference in conductance being larger when b is small).

According to the metabolic scaling theory, leaf metabolism (and therefore transpiration) is assumed to be independent of tree height (H) (West *et al.*, 1999). Accordingly, the leaf-specific hydraulic conductance (K_{LEAF}) should remain constant as a tree gets taller. In a tree, water moves from roots to leaves through

a set of hydraulic paths which are produced during different periods of growth (i.e. xylem rings or, more generically, xylem layers in the case of non-ring-bearing species).

The ring-to-ring connectivity (i.e. radial hydraulic conductivity) is probably limited (see further below), so that water flows along axial root-to-leaf hydraulic pathways primarily compartmentalized to each sapwood ring.

Two primary alternative hypotheses can be postulated on the anatomical adjustments that a tree can adopt with the allocation to current xylem biomass to compensate for the *H* effect and thus to maintain K_{LEAF} constant as it grows taller (Fig. 1): (H1) the hydraulic conductance of the stem apex-to-base pathway along the current (outermost) xylem layer (i.e. ring) (K_{NEW_XYLEM}) is maintained constant because either *a* or *b* (Equation 1) increase with *H*; and (H2) if neither *a* nor *b* (Equation 1) increases with *H*, the number of sapwood rings contributing to the total conductance (*NSWr*) increases with *H*.

In case inner sapwood rings are required to maintain K_{LEAF} independent of *H*, it can be further hypothesized that their number is affected by the Δ*H* effect mentioned above controlling the relative contribution of inner rings to the total hydraulic conductance (Fig. 2).

The axial length of a given inner xylem ring is shorter than the actual root-to-leaf distance by as much as the stem elongation since the year of formation of that ring. The production of new shoots distally implies additional resistances for water flowing in inner rings to pass, thus theoretically limiting their capacity to contribute to the hydraulic conductance at the whole-tree level. Consequently, other things being equal, the contribution of the water transport capacity of inner rings would be theoretically more limited in fast- than in slow-growing trees, since the longer young internodes of fast-growing trees would cumulate higher hydraulic resistances in series distal to the path length of the innermost rings. In this context, two alternative hypotheses can be postulated on the adjustments that trees can adopt to compensate for the negative Δ*H* effect on the hydraulic conductance of inner sapwood rings: (H3) *NSWr* is higher in trees with high Δ*H* compared with trees with low Δ*H* because more sapwood rings are required to attain a given hydraulic conductance; and (H4) *NSWr* is lower in trees with high Δ*H* compared with trees with low Δ*H* because the contribution of innermost rings to the total conductance becomes negligible, their metabolic maintenance thus would represent a 'wasteful' carbon cost, and the effective compensation for the Δ*H* effect is provided by a higher allocation to secondary growth (i.e. higher sapwood ring width, *SWrw*).

Ring-to-ring compartmentalization coupled with the lower conductance of inner sapwood rings would logically suggest that water flows at decreasing rates with increasing distance from the bark.

Empirical measurements support this prediction by showing that sap flow rate typically decreases with distance from the bark (from bark inwards) (Phillips *et al.*, 1996; Jiménez *et al.*, 2000; Gartner and Meinzer, 2005; Zhao *et al.*, 2018), to ultimately cease at the transition into the non-functional heartwood (Gebauer *et al.*, 2008; Beauchamp *et al.*, 2013). In this context, the contribution of inner rings to the total tree conductance may be affected by the radial resistance to water flow across the rings. However, there is not much information in the literature on the actual hydraulic pathway across the rings. A few studies reported low xylem radial conductivity and limited tracheary connections across adjacent rings in both angiosperms (Wason *et al.*, 2019) and conifers (Barnard *et al.*, 2013). Therefore, the axial hydraulic conductivity (i.e. conductance per unit of cross-sectional area and normalized for length) is probably orders of magnitude higher than the radial conductivity at any position along a given sapwood ring until its apical end, thus theoretically conferring an important hydraulic compartmentalization to the successive xylem layers (i.e. rings).

To test our hypotheses, we employed different integrated approaches, consisting of a detailed dataset with anatomical measurements taken at several positions along the stem of a mature Norway spruce and a mature European beech tree, to test H1 regarding the compensation mechanism for the *H* effect on K_{LEAF} (Fig. 1), a global database with empirical data of sapwood traits of conifer and angiosperm trees to test H2 regarding the compensation mechanism for the *H* effect on K_{LEAF} (Fig. 1) and H3 versus H4 regarding the compensation mechanism for the Δ*H* effect on the contribution of inner rings to the total hydraulic conductance (Fig. 2), and a numerical model of axial and radial xylem water transport to provide a validation test for our hypotheses.

Materials and methods

Different types of material, samples and analytical approaches were required to test our multifaceted hypothesis.

In order to test whether trees acclimate to increasing tree height by compensating for the negative *H* effect on the path length conductance (Fig. 1), we combined two different approaches.

Firstly, we carried out a detailed anatomical analysis on a conifer and a broadleaved tree to test whether the lumen diameter of xylem conduits from the stem apex to base is adjusted with increasing *H*. Secondly, we compiled a large dataset with our own and published data to test whether the number of sapwood rings (*NSWr*) increases with *H*. Notably, *NSWr* represents the sapwood turnover rate; that is, the time period from ring production to its transition into heartwood.

In addition, we used the compiled dataset to test the effect of stem elongation (Δ*H*) on *NSWr* and on the mean width of sapwood rings (*SWrw*) (Fig. 2).

Lastly, we developed a numerical hydraulic model based on the obtained anatomical data to predict the effect of *H* and Δ*H* on the hydraulic contribution of inner sapwood rings to the total conductance.

Vertical profiles of xylem conduit diameter

In order to test for the constancy of the allometric parameters *a* and *b* (Equation 1) during ontogeny or their scaling with tree height, we used our own dataset with detailed anatomical measurements at the ring level

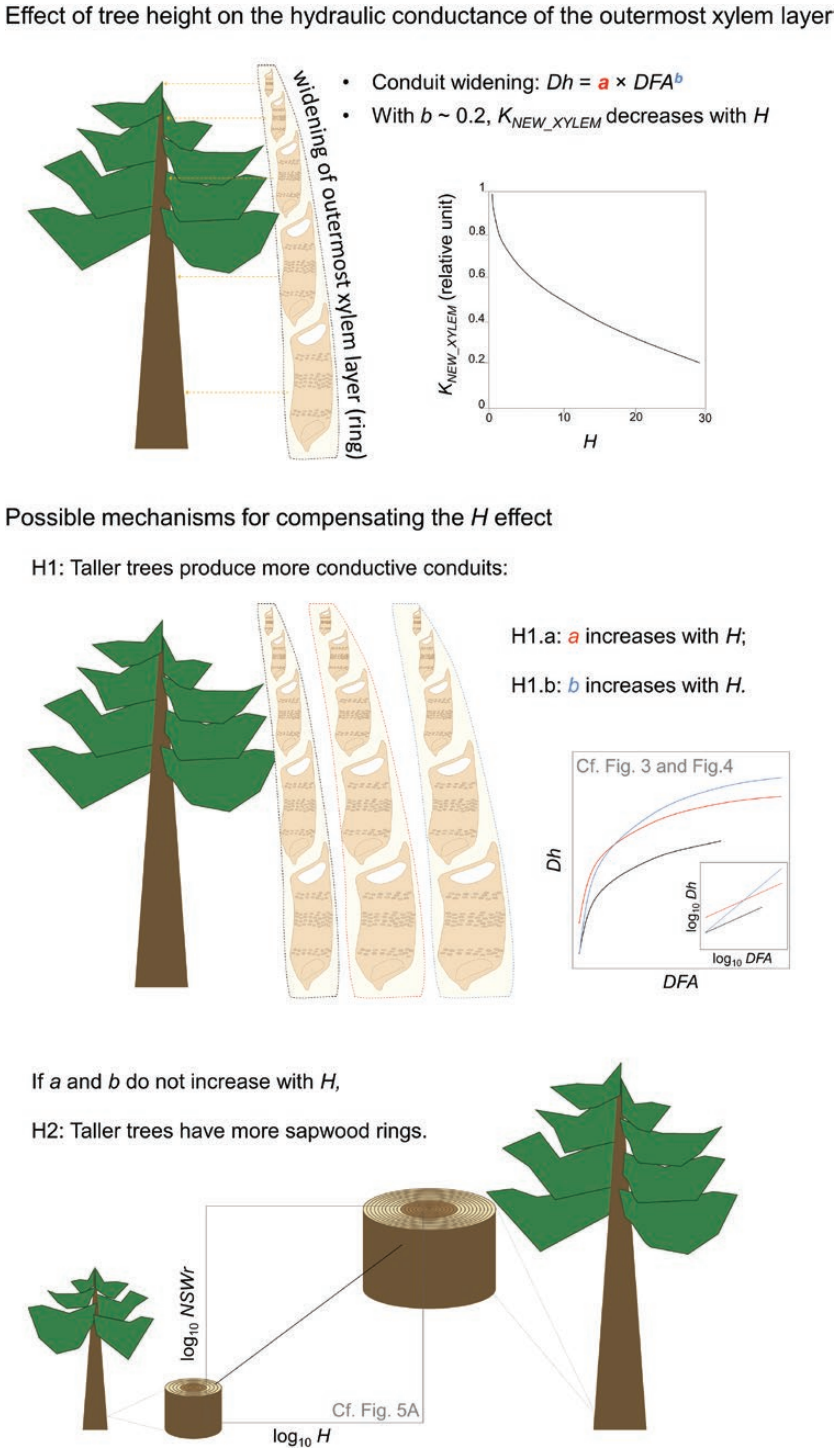

Fig. 1. Possible mechanisms of compensation for the effect of increasing height (*H*) to maintain a constant leaf-specific hydraulic conductance (K_{LEAF}) during the ontogenetic development of a tree. In the top panel it is shown that the total path conductance of the outermost xylem layer (i.e. ring: K_{NEW_XYLEM}) progressively decreases with increasing *H*. According to hypothesis H1, the conduit diameter (here expressed as *Dh*) increases with the distance from the stem apex (*DFA*) according to a power scaling ($Dh=a\times DFA^b$), whose parameter *a* (red line) or *b* (blue line) increases when a tree becomes taller (the black solid line represents the stem apex-to-base *Dh* pattern of the same tree at shorter *H*). According to hypothesis H2, *a* and *b* do not increase with *H*, whereas the number of sapwood rings (*NSWr*) increases with *H*.

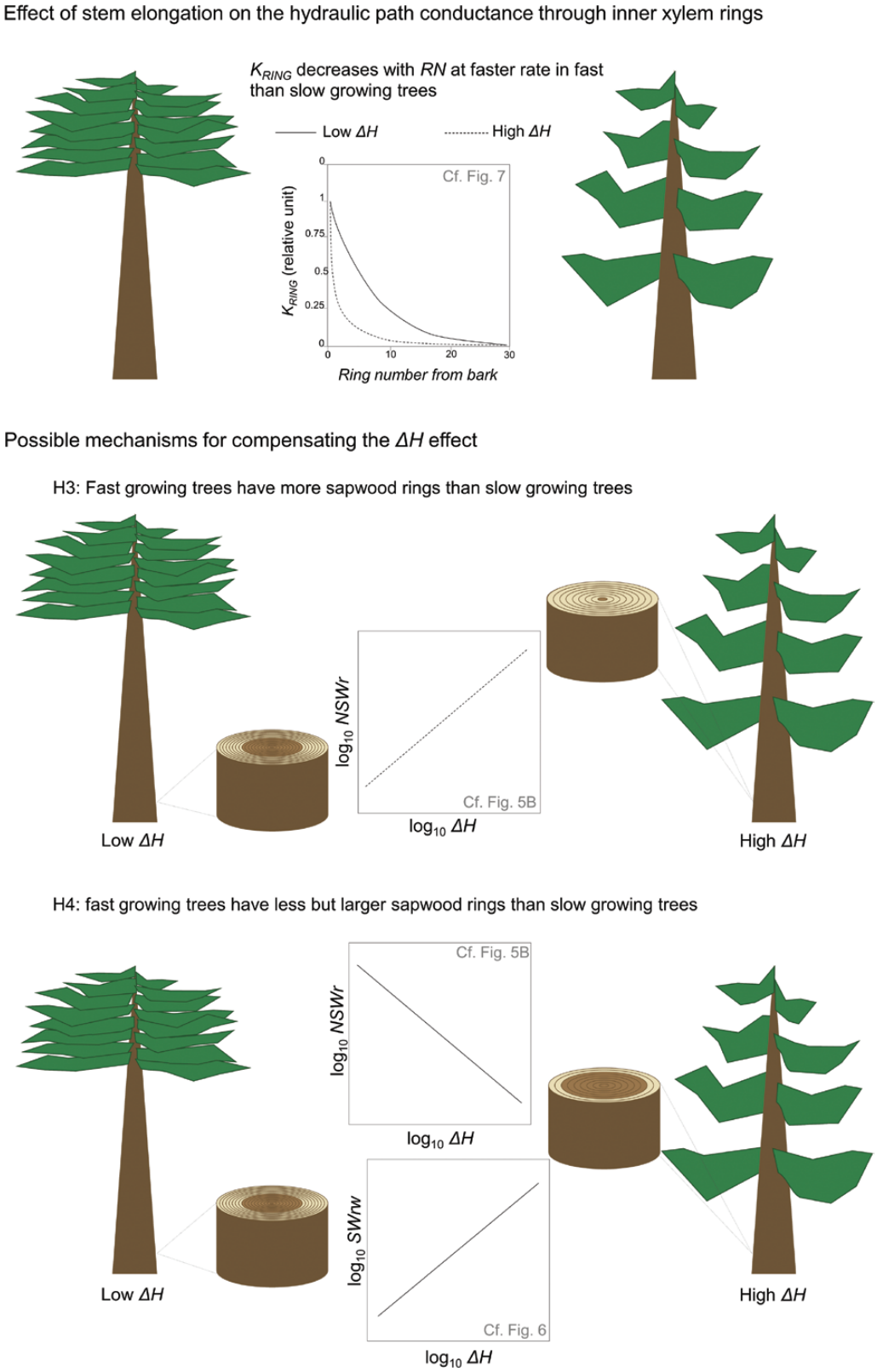

Fig. 2. Possible mechanisms of compensation for the effect of the stem elongation rate (Δ*H*) on the stem apex-to-base conductance of the hydraulic path through the different sapwood rings (K_{RING}). The top panel shows the variation in K_{RING} of the different rings numbered in the radial direction from bark to pith. The solid and dashed lines represent a tree with low and a tree with high Δ*H*, respectively. According to hypothesis H3, trees with high Δ*H* have a high number of sapwood rings (*NSWr*) to compensate for the low contribution of inner sapwood rings to the total leaf-specific hydraulic conductance (K_{LEAF}). According to hypothesis H4, trees with high Δ*H* have a low *NSWr* because of the low contribution of inner sapwood rings to K_{LEAF}, while effective compensation for the Δ*H* effect is provided by producing larger sapwood ring widths (*SWrw*).

from two mature trees, one conifer and one broadleaf, selected at two sites in the Eastern Italian Alps. A dominant Norway spruce (*Picea abies* Karst.) tree (PA) was felled in 2012 at a subalpine mixed stand located at Latemar (Bozen, Italy: 46°23′ latitude, 11°32′ longitude) at 1900 m asl, whereas a dominant European beech (*Fagus sylvatica* L.) (FS) was felled in 2013 in a pure even-aged stand located at Cansiglio (Belluno, Italy: 46°04′ latitude, 12°25′ longitude). Mean annual temperature and total annual precipitation at the sites are 4.7/6.6 °C and 950/1800 mm at Latemar/Cansiglio, respectively. The tree height (H) and diameter at 1 m from the ground (D) were H=26 m and D=35 cm for PA, and H=31 m and D=35 cm for FS. Tree age (222 years for PA and 140 years for FS) was assessed as the number of annual rings counted on the most basal stem disc (at 1 m from the ground). Discs used for dendro-anatomical analyses were extracted at different positions along the stem (at 1, 3, 5, 7, 9, 11, 13, 15, 17, 18, 19, 20, 21, 22, 23, 24, and 25 m from the ground, plus another seven discs along the last metre to the treetop for PA, at 2, 7, 8, 12, 16, 20, 22, 24, 25, 26, 27, and 28 m from the ground, plus another 10 discs along the last 3 m to the treetop for FS).

From each sampled disc, a radial 1 cm wide and 1 cm thick wooden block spanning from the pith to the outermost ring was extracted. Tree-ring width (*RW*) was measured to the nearest 0.01 mm (CCTRMD model, Aniol, 1987) and cross-dated with the other discs belonging to the same individual to assign the correct calendar year of formation, following standard dendrochronological protocols (Stokes and Smiley, 1968). Wooden sectors were then split into smaller trapezoidal blocks paying attention to creating an overlap between successive blocks to avoid missing rings. Thin sections of 15 µm thickness were then cut with a rotary microtome (Leica RM2245, Leica Biosystems, Nussloch, Germany), stained with safranine (1% in distilled water), and permanently fixed on glass slides with Eukitt (BiOptica, Milan, Italy). Overlapping images (~25%) of the sections taken at ×100 magnification with a Nikon Eclipse 80i microscope (Nikon, Tokyo, Japan) were stitched together with PTGui (New House Internet Services B.V., Rotterdam, the Netherlands), and then analysed with ROXAS (von Arx and Carrer, 2014). Ring boundaries were outlined manually, and then the software automatically measured for each ring the mean width (*RW*) and the lumen area of all vascular elements (tracheids for spruce, vessels and possibly some indistinguishable imperforate tracheary elements for beech), from which the hydraulically weighted lumen diameter was automatically calculated (Kolb and Sperry, 1999) ($Dh=\Sigma d_i^5/\Sigma d_i^4$, where d_i is the diameter of the i-conduit). In synthesis, all vascular conduits along a pith-to-bark wooden stripe of 1 cm width were measured for each disc of both sampled trees.

The time series of *RW* automatically measured by ROXAS on each core section was validated against that measured with CCTRMD to assign the correct calendar year of formation (n) of all the rings.

The total tree height at the n-year (H_n) was retrospectively reconstructed as:

$$H_n = h_k + \frac{l_{(k/k+1)}}{N_k - N_{k+1}} \cdot CA_n \qquad (2)$$

where h_k is the distance from the ground of the k-disc, N_k the number of rings of the k-disc, $l_{(k/k+1)}$ the distance between the k-disc and that sampled above (k+1), and CA_n the cambial age of the n-ring. The actual distance from the apex of the n-ring of the k-disc (hereafter distance from contemporary apex, *DCA*) was then estimated as:

$$DCA_n = H_n - h_k. \qquad (3)$$

Since the number of rings decreased in discs sampled at higher positions along the stem, the number of axial points along a given ring decreased for younger tree ages.

Tree growth and sapwood properties

In order to test whether the number of sapwood rings at the stem base (*NSWr*) varies with tree height and the stem elongation rate (ΔH), we compiled a large dataset of biometric and tree ring data composed of our own measurements (collected from several sites across the Alps) and data from the global biomass and allometry database (BAAD) (Falster *et al.*, 2015).

A total of 503 trees from four species (*Abies alba* Mill., *Picea abies* Karst., *Pinus cembra* L., and *Larix decidua* Mill.) were sampled from 78 stands across the Eastern Italian Alps (45°08′–46°09′ latitude, 10°04′–13°07′ longitude), ranging >1000 m in elevation (1050–2200 m asl), with contrasting stand attributes (pure and mixed, even- and uneven-aged, managed and unmanaged) and environmental settings (temperature, elevation, precipitation range, soil type, and slope). For each tree, we measured the total tree height (H) with a hypsometer (TruPulse, Denver, CO, USA) and the diameter at breast height (*Dbh*) with a diameter tape. Two cores were extracted at breast height and the sapwood boundary was marked immediately according to chromatic transition into heartwood (e.g. in *Larix* or *Pinus* spp.) or to its translucency, due to the presence of water, against direct light (Quiñonez-Piñón and Valeo, 2018) (e.g. in *Abies* or *Picea* spp.). Tree age was estimated by counting the total number of rings of cores extracted at breast height. In off-centre cores, we fitted a geometric pith locator to the innermost rings to estimate the distance to the theoretical pith and number of missing rings (Duncan, 1989). Sapwood rings were then counted (*NSWr*), their width measured as described before, and the mean sapwood ring width (*SWrw*) calculated. Mean stem elongation rate was assessed as $\Delta H = H/\text{age}$.

From the BAAD dataset (Falster *et al.*, 2015), only trees with the concomitant presence of the following variables were selected for our analyses: age, diameter at breast height (*Dbh*; basal stem diameter was used when *Dbh* information was missing), tree height (H), and sapwood area (*ASW*). The filtered dataset comprised 562 trees from five angiosperm (*Eucalyptus delegatensis* R.T. Baker, *Eucalyptus grandis* W. Hill, *Eucalyptus nitens* H. Deane and Maiden, *Eucalyptus urophylla* × *grandis*, and *Populus tremuloides* Michx) and five conifer species [*Picea mariana* (Mill.) BSP, *Pinus banksiana* (Lamb.), *Pinus ponderosa* Douglas, *Pinus sylvestris* L., and *Pseudotsuga menziesii* (Mirb.) Franco[.

ΔH and *SWrw* were estimated as H/age and *Dbh*/(2×age), respectively. The heartwood diameter (*DHW*) was calculated as $2\times(BA-ASW)/\pi^{0.5}$, where *BA* is the stem basal area, calculated as $BA=\pi\times(Dbh/2)^2$. Sapwood width (*WSW*) was then calculated as $WSW=(Dbh-DHW)/2$. Lastly, the number of sapwood rings (*NSWr*) was estimated as $WSW/SWrw$.

The list of variables used in this study is reported in Table 1.

Statistical analyses

Allometric relationships were analysed on $\log_{10}$-transformed data. Bayesian linear models (R package brms: Bürkner, 2017) were used to

Table 1. List of variables: growth and sapwood traits

	Symbol (units)	Variable
Growth traits	Age (years)	Tree age
	Dbh (cm)	Diameter at breast height
	H (m)	Tree height
	DCA (m)	Distance from contemporary apex
	ΔH (cm)	Mean annual height increment
Sapwood traits	*NSWr* (#)	Number of sapwood rings at *Dbh*
	SWrw (mm)	Mean width of sapwood rings at *Dbh*

test for fixed effects and interactions on the target dependent variables. Models were evaluated using the leave-one-out cross-validation (LOO) method (Bürkner, 2017). When the difference in the expected log pointwise predictive density (elpd) of two models is <4 units, we choose the simplest. All analyses were performed with the software R version 4.1.3 (R Development Core Team, 2022).

In order to test for the ontogenetic variability of both the allometric constant (a) and the exponent (b) of Equation 1, we tested for the fixed effect of H on the y-intercept and slope of the linear relationship between $\log_{10}Dh$ and $\log_{10}DCA$, respectively. H was used either as numeric ($\log_{10}H$) or a factor variable (with H approximated to integer numbers, thus resulting in H classes of 1 m).

Furthermore, we tested for the independent path length effect of H or ΔH on $NSWr$, using a linear model with $\log_{10}NSWr$ as the dependent variable, $\log_{10}H$ or $\log_{10}\Delta H$, ΔH_{CLASS} or H_{CLASS} (used as factor variables), and interactions ($\log_{10}H\times\Delta H_{CLASS}$ or $\log_{10}\Delta H\times H_{CLASS}$) as independent variables. Lastly, we tested for the fixed effects of $\log_{10}\Delta H$, division (Conifers/Angiosperms), and their interaction on $\log_{10}SWrw$.

Hydraulic model

We built a novel numerical model with two dimensions (i.e. axial and radial direction). The structural and functional xylem properties in the tangential direction (i.e. the third dimension) were assumed to be homogeneous and were not considered in the model. The model was designed to simulate the contribution of each sapwood ring (assuming all conduits to be functional) to total tree hydraulic conductance, considering both the axial and radial hydraulic pathways from stem base to leaves. The model tree dimensions and parameter values used in the different simulations are reported in Table 2. The model was divided into N times M numerical elements in cylindrical coordinates as represented in Supplementary Fig. S1. The axial height of each element was tree height (H) divided by N, and the radial width of each element was calculated so that each ring had the same cross-sectional area. Water was lost by transpiration only from the topmost element i=N and j=M. The axial conductance between different elements (K_{ax}) of each element was calculated as

$$K_{\mathrm{ax}_{i-1,j\_i,j}} = \frac{k_{\mathrm{ax}_{i-1,j\_i,j}}}{\Delta\, x_{i-1,j\_i,j}} \times A_{\mathrm{ax}_{i-1,j\_i,j}} \quad (4)$$

where k_{ax} is the area-specific axial hydraulic conductivity, A_{ax} is the cross-sectional area between two elements, and Δx is the distance between two adjacent elements. The radial conductance (K_{RAD}) between two radial elements j–1 and j is

$$K_{\mathrm{RAD}_{i,j-1\_i,j}} = \frac{k_{\mathrm{RAD}_{i,j-1\_i,j}}}{\Delta_{x_{i,j-1\_i,j}}} \times A_{\mathrm{RAD}_{i,j-1\_i,j}} \quad (5)$$

where k_{RAD} is the area-specific radial hydraulic conductivity, and A_{RAD} is the longitudinal area between two numerical elements.

The axial hydraulic conductivity (k_{ax}) is calculated from the conduit radius (d), which is made to scale with distance from the contemporary apex (DCA):

$$k_{\mathrm{ax}_{i,j}} = a \times d^4 = a \times \left(DCA^b\right)^4 \quad (6)$$

where a and b are the allometric constant and exponent of the axial scaling of conduit diameter (Equation 1). Although no conduit number is explicitly assigned for each i,j element in our model, this corresponds to having no conduit furcation in the model. Radial hydraulic conductivity (k_{RAD}) was assumed to have the same constant value everywhere (in the base case k_{RAD}=3 × 10^{-12} m^3 m^{-1} s^{-1} Pa^{-1}: Barnard *et al.*, 2013), although alternative scenarios were also explored.

Table 2. List of model parameters

Parameter	Symbol (units)	Value
Tree height	H (m)	2
		4
		8
		16
		32
		64
Radial hydraulic conductivity	k_{RAD} (m^3 m^{-1} s^{-1} Pa^{-1})	3 × 10^{-11}
		3 × 10^{-12} (base case)
		3 × 10^{-13}
		3 × 10^{-14}
		3 × 10^{-15}
Axial hydraulic conductivity at stem apex for b=0.15	k_{ax} at i=j (m^2 Pa^{-1} s^{-1})	0.8 × 10^{-9}
Xylem conduit widening coefficient	b	0
		0.15
		0.3
Number of numerical elements used in the simulations (=tree age)	N, M (N=M)	20
		40
		80
Stem diameter at breast height	Dbh (cm)	24
		Dbh=0.4×H

The total tree conductance represents the outcome of both the axial and radial hydraulic properties in 2D at the whole-tree level, calculated by progressively increasing the number of axially conducting sapwood rings starting from the outer one and going inward (K_{CUM} and rK_{CUM}, i.e. relative K_{CUM} relativizing all values to a maximum of 1).

We also calculated the stem apex-to-base conductance of each ring (K_{RING}: i.e. the combined conductance of the ring and of that of younger shoots distally until the stem apex), by subtracting whole-tree values differing for one additional inner ring (i.e. K_{RING}=$K_{CUM,RN=i+1}$–$K_{CUM,RN=i}$). Given that leaf area dynamics were not modelled, the model assumes a constant leaf area and thus constant total tree conductance.

Height growth rate (ΔH) was considered in the model parameterization so that the length of each axial annual stem increment was the total tree height divided by its age. The number of the numerical elements M and N (where M=N) was made to match tree age (i.e. each numerical element represented 1 year's growth in both axial and radial dimensions). The difference in structure between the slow- and fast-growing trees and the base case tree is depicted in Supplementary Fig. S1.

This hydraulic model differs from the original pipe model of Shinozaki *et al.* (1964) as it employs the actual variation of xylem anatomy (and thus hydraulic properties) across the sapwood. Therefore, in our 2D model the unit leaf is not simply connected to a unit pipe, but the number of sapwood pipes varies according to the variation of their hydraulic efficiency with H and ΔH: the unit leaf is therefore connected to a radial file of pipes (xylem rings). Accordingly, the model does not account for ontogenetic changes in leaf area, which would translate into an increase of sapwood area (not included in the model).

Results

Axial and radial patterns of xylem conduit diameters

Axial and radial patterns of xylem conduit diameters were analysed to test our hypothesis H1 for the compensation mechanism for the negative effect of H on K_{LEAF} (Fig. 1). Firstly, we described the variation in Dh with the axial and radial position in the stem in both Norway spruce and European beech (Figs 3, 4). The vascular elements formed in a given year were larger at the stem base and 'tapered' (i.e. became narrower) with height (coloured lines in Figs 3A and 4A). In each stem disc, Dh increased with cambial age (i.e. radially from pith to bark), showing a steep interannual increase during the first years followed by a period of minor Dh variation (e.g. at the stem base: Figs 3C, 4C).

Changing perspective, when the Dh of each ring in each disc was related to the distance to the contemporary stem apex (DCA), a strong convergence towards an invariant axial scaling emerged (Figs 3B, 4B). A linear regression fitted the $\log_{10}$-transformed data of Dh versus DCA well (Supplementary Table S1). The slope did not change with varying tree height (H) in either spruce and beech (b=0.14 and b=0.23, respectively: Supplementary Table S1). In contrast, H significantly affected the γ-intercept (Figs 3E, 4E; Supplementary Tables S1, S2). This indicated that the Dh at the stem apex (i.e. at DCA=1 cm, cf. Fig. 3B and E and Fig. 4B and E) slightly increased or decreased with H in spruce and beech, respectively (Table 3; Supplementary Table S2). The magnitude of variation was in the order of ~15 µm in beech, and only in the order of ~5 µm (but becoming negligible approximately for H >5 m) in spruce. These results did not support hypothesis H1 of Fig. 1 that a tree can maintain a constant K_{LEAF} while growing taller by increasing the allometric parameter a or b of the axial scaling of Dh with DCA (Equation 1) to compensate for the negative H effect on the total hydraulic conductance.

Growth-related patterns in the number and width of sapwood rings

The global dataset was used to test the hypothesis that the H effect on K_{LEAF} is compensated by a higher number of sapwood rings contributing to the total hydraulic conductance (hypothesis H2 of Fig. 1). Empirical data supported this hypothesis, as the number of sapwood rings ($NSWr$) increased with H (Fig. 5A; Supplementary Table S3A). Data were separated into groups of different annual H increment (ΔH), in order to account for the ΔH effect on the conductance of inner sapwood rings and thus on $NSWr$. Notably, groups were displayed in descending γ-intercept with increasing ΔH (consistent with Fig. 5B).

The possible compensation mechanism for the ΔH effect on the total hydraulic conductance (Fig. 2) was specifically investigated by analysing the relationships between $NSWr$ and ΔH, and between the mean ring width of sapwood rings ($SWrw$) and ΔH. For the relationship between $NSWr$ and ΔH, data were divided into groups of different H to account for the effect of this parameter on $NSWr$. As a result, $NSWr$ was inversely related to ΔH (Fig. 5B; Supplementary Table S3B), with groups being displayed in ascending γ-intercept with increasing H (consistent with Fig. 5A).

Moreover, $SWrw$ significantly increased with ΔH, with conifers producing wider rings than angiosperm trees at a given ΔH (Fig. 6; Supplementary Table S3C).

These results supported the hypothesis that the negative ΔH effect on the conductance of inner sapwood rings is compensated by producing larger $SWrw$ while reducing $NSWr$ with increasing ΔH (according to hypothesis H4 of Fig. 2).

Effects of tree height, stem elongation rate, ring width, radial conductivity, and scaling exponent (b) of conduit widening scaling on the conductance and number of sapwood rings according to the hydraulic model

Analyses with the hydraulic model gave further insights into the processes controlling the observed empirical trends. Model simulations revealed that the marginal gain in total conductance of adding one inner sapwood ring rapidly decreases moving from the outermost ring (ring number RN=1) towards older rings (ring number RN=40; Supplementary Fig. S2). The pattern of relative variation in the cumulative hydraulic conductance (rK_{CUM}) with RN was affected by both total tree height (H) and stem elongation rate (ΔH). That is, inner rings contribute relatively more to the total sapwood conductance either with increasing H (Fig. 7A) or with reduced ΔH (Fig. 7C). Furthermore, the radial profile of rK_{CUM} was substantially independent of the average ring width ($SWrw$) (cf. red circles and inverted grey triangles in Fig. 7C).

Keeping constant two of the three parameters H, ΔH, and $SWrw$, to examine the marginal effects across all model combinations, the model predicted that the total xylem conductance (K_{TOT}=maximum K_{CUM}) declined with increasing H (data not shown), and increased either with increasing $SWrw$ (cf. red circles and inverted grey triangles in Fig. 7B) or with decreasing ΔH (Fig. 7B). The example of Fig. 7B shows that for a tree of height H=8 m, K_{TOT} depends on the balance between primary (ΔH) and secondary growth ($SWrw$). Notably, the simulations revealed that K_{TOT} can remain close to constant despite reduced ΔH and $SWrw$ (i.e. despite reduced allocation to both primary and secondary growth), because reduced ΔH facilitated the retention of inner sapwood rings via reduced resistances (cf. yellow diamonds and inverted grey triangles in Fig. 7B).

Furthermore, the model revealed that the radial profiles of K_{CUM} were sensitive to the input parameters of the widening exponent (b) and radial conductivity (k_{RAD}) (Fig. 8). Specifically, the contribution of inner rings to K_{TOT} decreased rapidly when conduit widening is steep (i.e. high b values: Fig. 8A). Lower k_{RAD} led to lower K_{TOT} (Fig. 8B) and to a lower contribution of inner rings to K_{TOT} (Fig. 8C). However, the

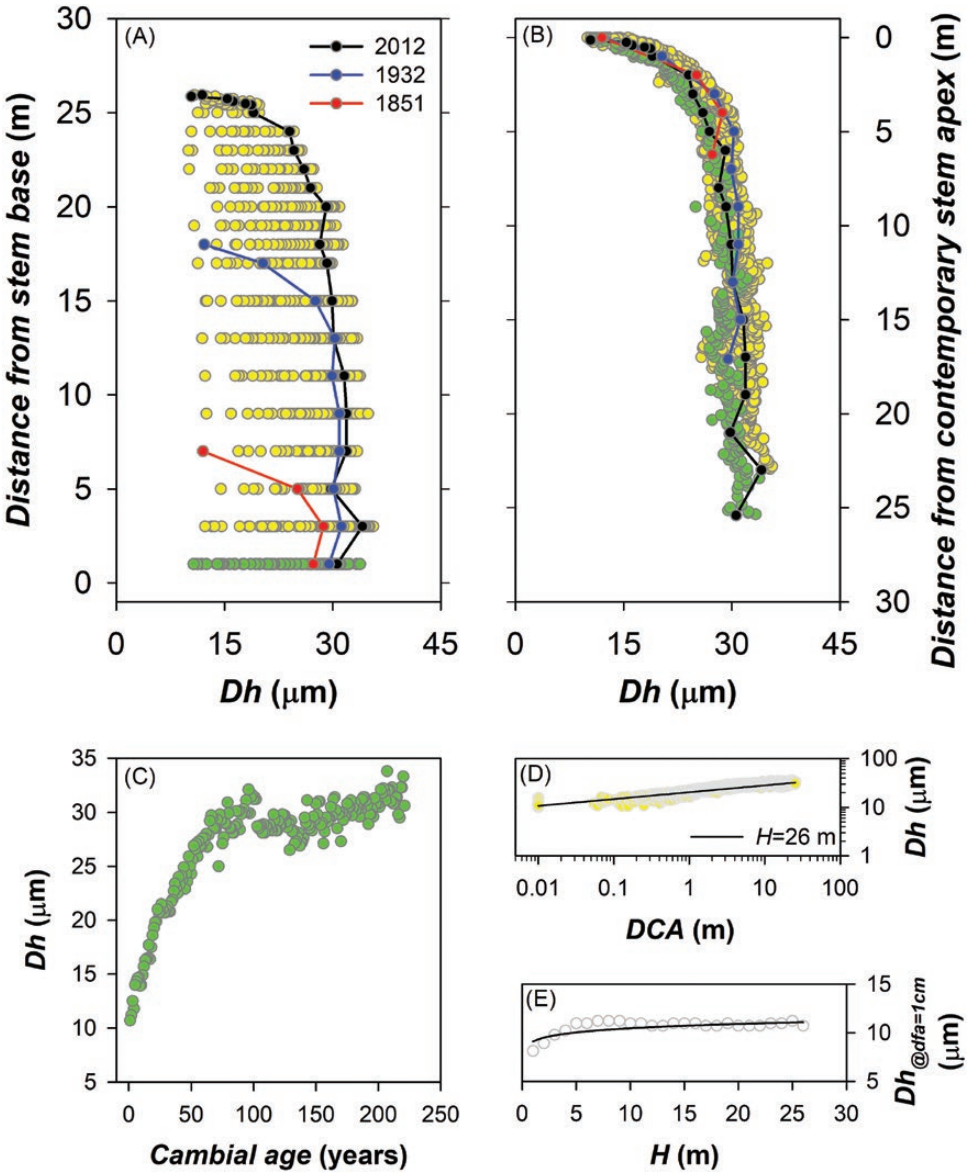

Fig. 3. Intra-tree variation of tracheid *Dh* in a 222-year-old Norway spruce (*P. abies*) tree of *H*=26 m. (A) Range variation of *Dh* in all the annual rings of the discs extracted at different heights along the stem. Coloured lines outline the 'acropetal tapering' of *Dh* along example annual rings (Sanio's second law) (black, 2012; blue, 1932; red, 1851). (B) The same *Dh* data as in (A) are plotted against the distance to the height position that the stem apex had in the corresponding year (distance from contemporary apex, *DCA*). Green circles in (A), (B), and (C) represent the same *Dh* data from the most basal stem disc. (C) Radial variation of *Dh* with cambial age (i.e. from pith to bark: Sanio's first law) in the most basal stem disc. (D) Relationship of *Dh* versus *DCA* expressed on a log–log scale, with the solid line outlining the estimated scaling for years with H_{CLASS}=26 m (Supplementary Table S2A). (E) Variation of *Dh* at the fixed distance from the apex of 1 cm ($Dh_{@dfa=1\ cm}$) with increasing H_{CLASS}. The solid line is according to the model of Supplementary Table S1A keeping *DCA*=1 cm.

effect of k_{RAD} rapidly saturated above the highest value employed in the parameterization.

The transition of the oldest sapwood ring into heartwood was arbitrarily assumed to occur with a marginal increase in rK_{CUM} <0.3 % (i.e. $rK_{CUM\_RN=n}$<0.003×$rK_{CUM\_RN=n-1}$). The model predicted that the variation in *NSWr* was positively related to *H* (Fig. 5A; Supplementary Fig. S3) and negatively related to Δ*H* (Fig. 5B; Supplementary Fig. S3). The predicted relationships were sensitive to the parameter k_{RAD} (Fig. 8C) and especially to the widening scaling exponent (*b*) (Fig. 8A). In order to account for the possible variability in *b* among trees, the hydraulic model was run under three scenarios. Under the condition of *b*=0, the model predicted the largest number of sapwood rings, with *NSWr* scaling at a faster rate with *H* compared with empirical data (Supplementary Fig. S3A). Under *b*=0.15, the model predicted the scaling of *NSWr* with *H* well, especially for trees with low Δ*H* (Fig. 5A). In contrast, model simulations implementing *b*=0.3 predicted the lowest number of sapwood rings, and a rather flat scaling of *NSWr* with

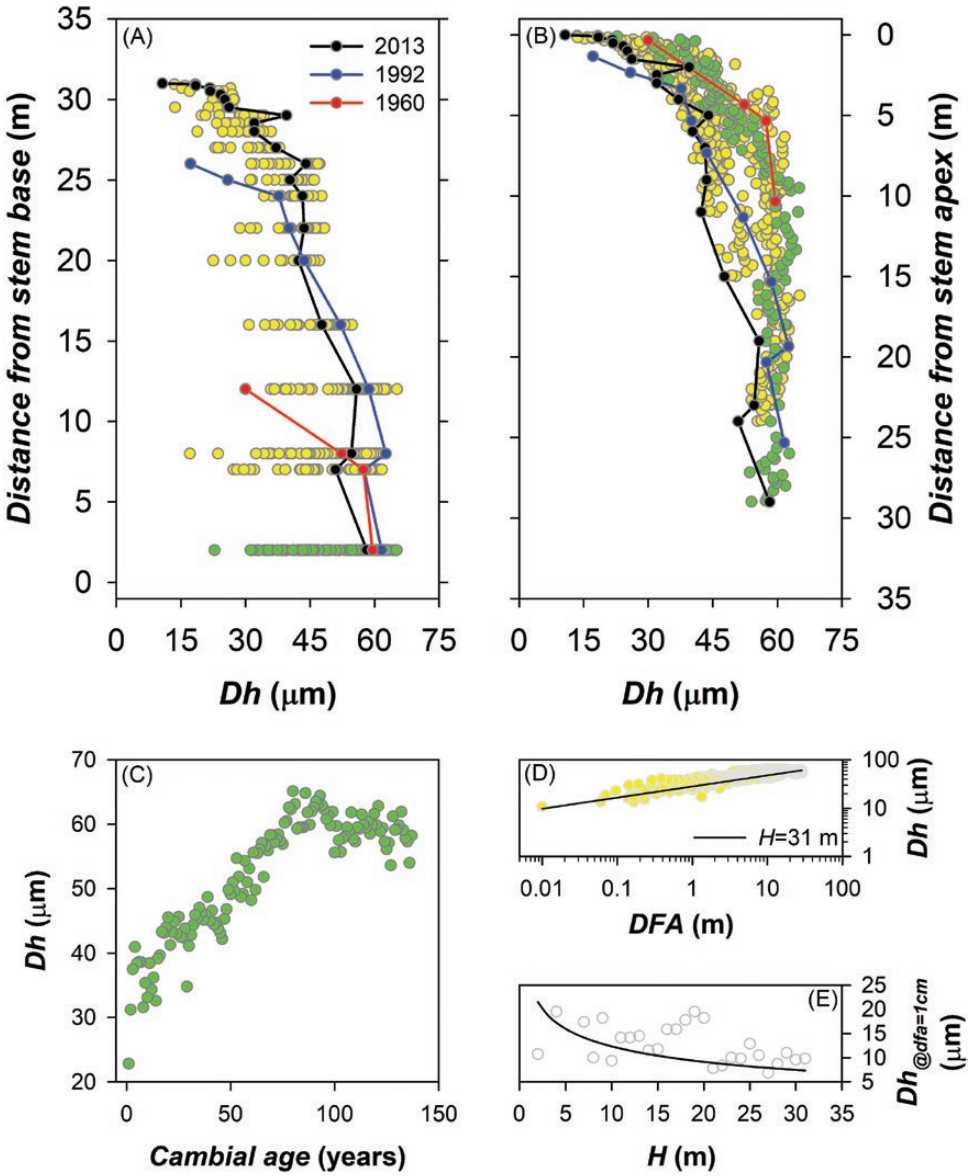

Fig. 4. Intra-tree variation of vessel *Dh* in a 140-year-old *F. sylvatica* tree of *H*=31 m. (A) Range variation of *Dh* in all the annual rings of the discs extracted at different heights along the stem. Coloured lines outline the 'acropetal tapering' of *Dh* along example annual rings (Sanio's second law) (black, 2013; blue, 1992; red, 1960). (B) The same *Dh* data as in (A) are plotted against the distance to the height position that the stem apex had in the corresponding year (distance from contemporary apex, *DCA*). Green circles in (A), (B), and (C) represent the same *Dh* data from the most basal stem disc. (C) Radial variation of *Dh* with cambial age (i.e. from pith to bark: Sanio's first law) in the most basal stem disc. (D) Relationship of *Dh* versus *DCA* expressed on a log–log scale, with the solid line outlining the estimated scaling for years with H_{CLASS}=31 m (Supplementary Table S2B). (E) Variation of *Dh* at the fixed distance from the apex of 1 cm ($Dh_{@dfa=1\ cm}$) with increasing H_{CLASS}. The solid line is according to the model of Supplementary Table S1B keeping *DCA*=1 cm.

H, especially for trees with high Δ*H*, thus more consistent with empirical data in that range (Supplementary Fig. S3B).

Discussion

In this study, we used different analytical approaches to provide a general explanation for the transition of sapwood into heartwood based on biophysical principles of water transport. Our results provided support for the hypothesis that a tree can maintain a broadly constant leaf-specific conductance (K_{LEAF}) while getting taller because the residual negative *H* effect on K_{LEAF} that conduit widening alone cannot completely eliminate is likely to be compensated by a higher number of sapwood rings (*NSWr*). The hydraulic model suggested that an additional path length component (i.e. the stem elongation rate, Δ*H*) affected the contribution of the inner sapwood rings to the whole-tree hydraulic conductance, and provided a biophysical explanation for the transition of sapwood into

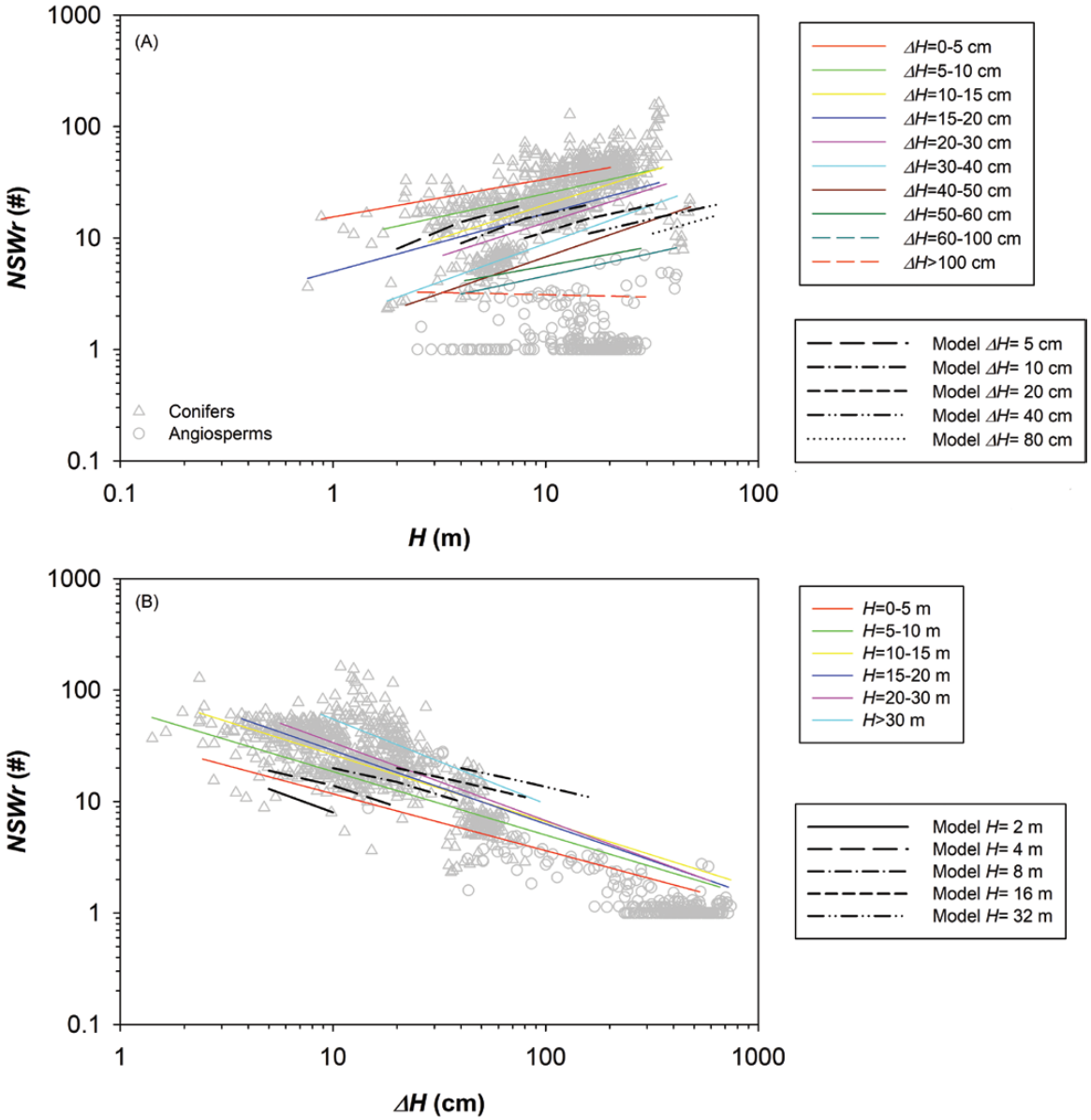

Fig. 5. Path length-related variation in the number of sapwood rings (*NSWr*). (A) Relationship between *NSWr* and tree height (*H*) assessed for different classes of annual stem height increment (ΔH=cm year^{-1}). Symbols represent conifers (triangles) and angiosperms (circles). (B) Relationship between *NSWr* and ΔH assessed for different *H* classes. Symbols represent conifers (triangles) and angiosperms (circles). Fitting lines are according to Supplementary Table S3B. Black lines represent the model predictions under the scenario of conduit widening scaling of *b*=0.15.

heartwood (and thus for the *NSWr*) to occur when the marginal increase in the total sapwood conductance caused by one additional ring becomes negligible. Data from the global dataset showed that trees with high ΔH compensate for the ΔH effect by maintaining few but large sapwood rings.

No adjustments in conduit widening can compensate for the H *effect*

Results from our detailed anatomical stem analysis unambiguously revealed that the vascular cambium produced xylem conduits with diameter strongly dependent on the distance from the apex (Figs 3, 4). However, our measurements did not support the hypothesis that the *H* effect would be effectively compensated by the increase in the widening parameters *a* or *b* with increasing *H* (hypothesis H1 of Fig. 1), as recently suggested (Echeverría *et al.*, 2019; Olson *et al.*, 2021). The *P. abies* and the *F. sylvatica* trees showed different values of *b* (0.14 and 0.22, respectively), but in the range of exponents commonly reported in the literature (Anfodillo *et al.*, 2013), and the observed invariance of *b* with *H* is in agreement with other less detailed studies (Weitz *et al.*, 2006; Prendin *et al.*, 2018b). In addition, in

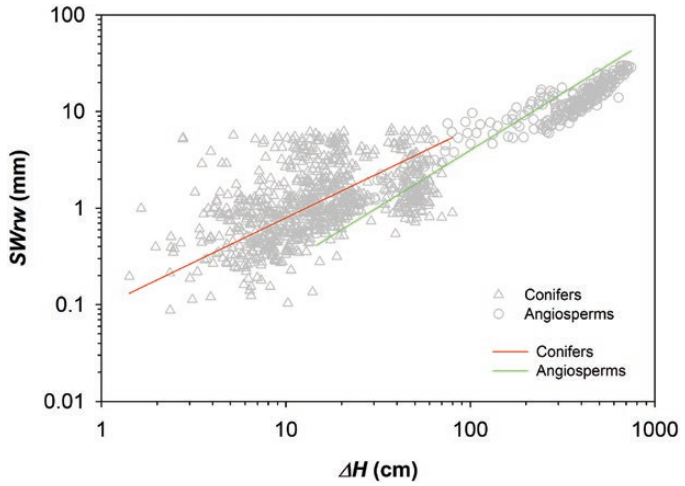

Fig. 6. Relationship between mean width of sapwood rings (*SWrw*) and mean annual height increment (Δ*H*) for both conifers (triangles) and angiosperms (circles). Fitting lines (red for conifers and green for angiosperms) are according to Supplementary Table S3C.

P. abies, the variation in *a* was negligible when *H* was greater than ~5 m (<1 μm), consistent with other intraspecific investigations reporting only marginal variations, if any, in *a* among conifer trees of different sizes (Prendin *et al.*, 2018a, b; Williams *et al.*, 2019CJML_BIB_J_0059). In *F. sylvatica*, we observed an overall decrease in *a* with *H* (of ~15 μm). These results contrast with other studies reporting a significant *Dh* increase at the stem apex (corresponding to the *a* parameter of Equation 1) with *H*, but either the assessed relationship was interspecific (Olson *et al.*, 2018) or no precise distance from the apex was reported in the methods (Echeverría *et al.*, 2019).

Although species-specific differences in *b* (varying from 0.1 to 0.4 according to the literature: e.g. Petit *et al.*, 2011; Williams *et al.*, 2019) would change the impacts of these residual path length effects at the ring level (Becker *et al.*, 2000; Petit and Anfodillo, 2009), the contribution of inner rings to the total sapwood conductance would become essential to fully compensate for the hydraulic limitations imposed by *H* on K_{LEAF} (hypothesis H2 of Fig. 1).

The effects of H *and* ΔH *on the conductance of sapwood rings*

The numerical model of water transport within and across xylem rings was used to physiologically characterize the independent effects of *H* and Δ*H* on the contribution of inner sapwood rings to total sapwood conductance.

The model predicted the variation in marginal ring conductance (K_{RING}) with ring age (i.e. ring number from the outermost one ring, *RN*) (Supplementary Fig. S2) under the effect of varying tree height (*H*) (Fig. 7A) and annual increment of stem height (Δ*H*) (Fig. 7C). Specifically, path length resistance cumulates less than linearly with distance from the apex (Becker *et al.*, 2000; Petit and Anfodillo, 2009); therefore, the difference in K_{RING} between adjacent

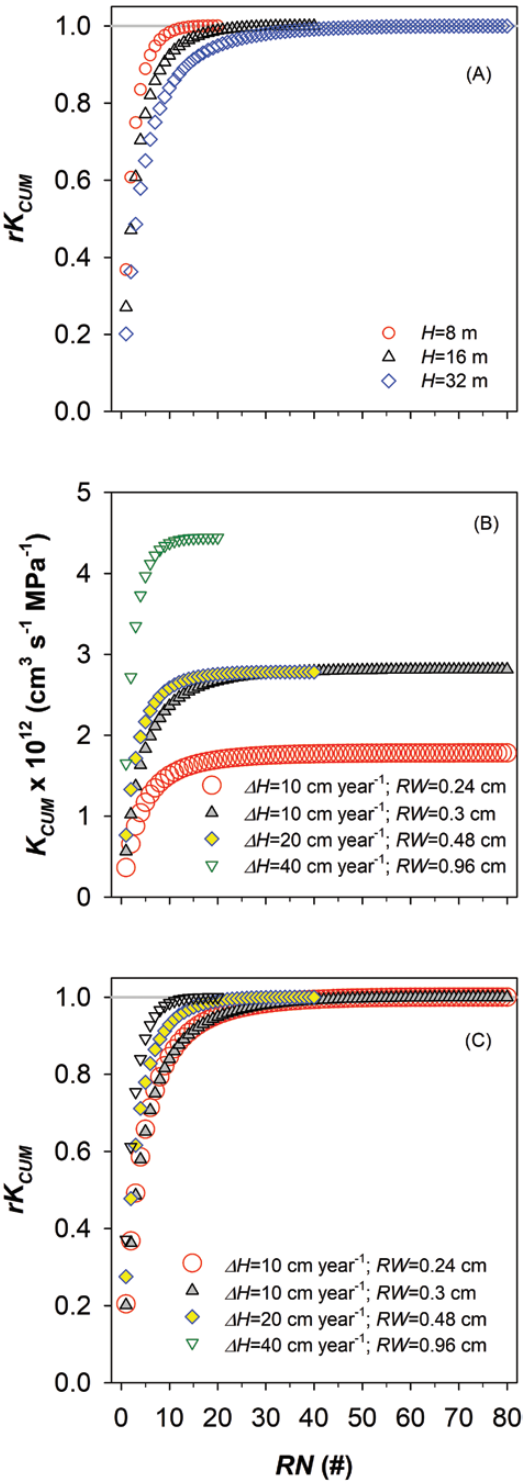

Fig. 7. Variation in the cumulative plant conductance (K_{CUM}: B) and in the relative K_{CUM} (rK_{CUM}: A, C) with the ring number starting from the outermost one (*RN*) for simulations comparing: (A) trees with the same stem elongation rate (*H*=40 cm year^{-1}) and different height and ring width (red circle: *H*=8 m, *RW*=1.2 cm; black triangle: *H*=16 m, *RW*=0.6 cm; blue diamond: *H*=32 m, *RW*=0.3 cm); (B, C) trees of the same height (*H*=8 m), but with different combinations of Δ*H* and *RW* (red circle: Δ*H*=10 cm year^{-1}, *RW*=0.24 cm; Δ*H*=10 cm year^{-1}, *RW*=0.3 cm; Δ*H*=20 cm year^{-1}, *RW*=0.48 cm; Δ*H*=40 cm year^{-1}, *RW*=0.96 cm).

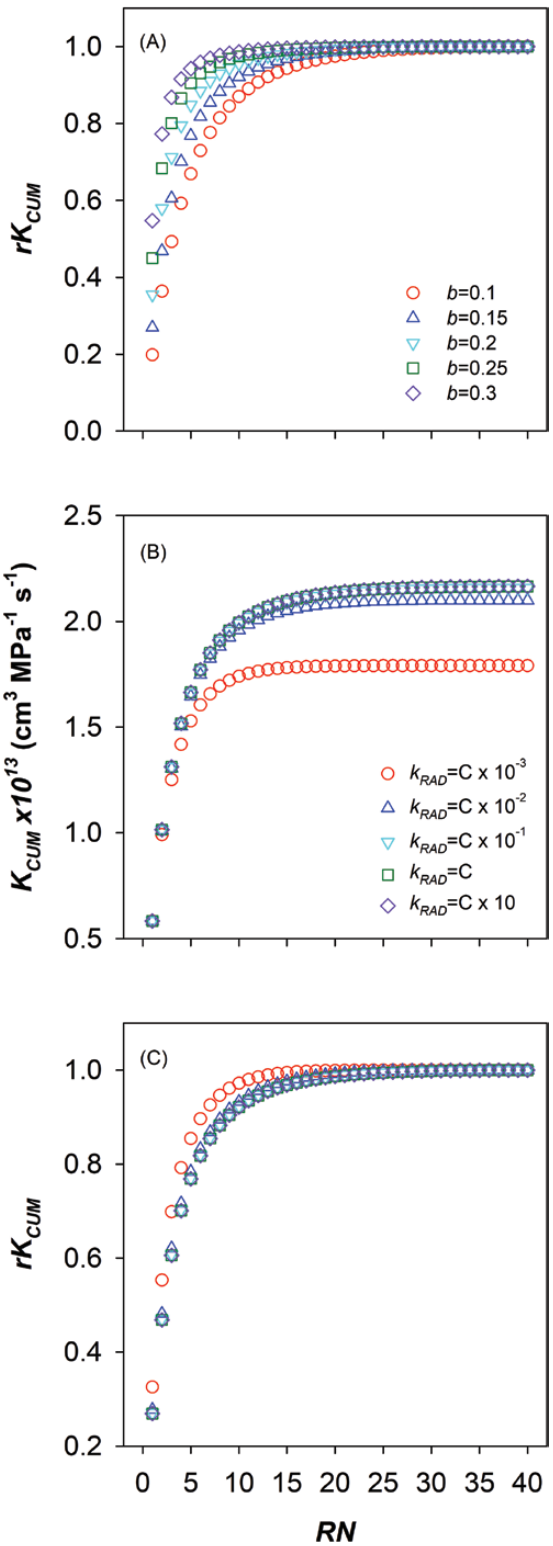

Fig. 8. Effects of the conduit widening exponent (*b*: A) and of the parameter of radial conductivity (k_{RAD}: B, C) on the variation in the cumulative xylem conductance (K_{CUM}, i.e. the cumulated contribution of the different rings, starting from the outermost one inward, to the total xylem conductance) (B) and in the relative K_{CUM} (rK_{CUM}: A, C) with the ring number (*RN*). The reference value for k_{RAD} in (B, C) is according to Barnard *et al.* (2013) (C=3 × 10^{-12} m^3 m^{-1} s^{-1} Pa^{-1}).

rings decrease with increasing *H*, making the contribution of older rings to the total conductance relatively larger in taller trees.

Analogously, since water flowing axially along inner rings has to pass through the additional axial resistances represented by the younger shoots distally before arriving at the leaves, and shoot resistance is proportional to its length, it follows that the contribution of inner rings to total tree hydraulic conductance decreases more rapidly when Δ*H* is high.

The predicted progressive decline of K_{RING} with ring number (Supplementary Fig. S2) is consistent with several studies reporting a radial decrease in sap flow rate with sapwood depth (Phillips *et al.*, 1996; Jiménez *et al.*, 2000; Gartner and Meinzer, 2005; Zhao *et al.*, 2018).

The compensation mechanisms for the H *and* Δ*H hydraulic effects on the sapwood conductance and the driver of sapwood/heartwood transition*

Data from the global sapwood database provided empirical support for our hypothesis and model predictions that the number of sapwood rings (*NSWr*) increases with increasing *H* to compensate for the negative *H* effect on K_{LEAF} (hypothesis H2 of Fig. 1). In addition, the hypothesis that the further hydraulic limitations imposed by Δ*H* on the conductance of inner rings would be compensated by maintaining more sapwood rings was rejected (hypothesis H3 of Fig. 2). Rather, the effective compensation mechanism for a high Δ*H* effect resulted in the production of larger sapwood rings while having a faster sapwood turnover (i.e. reducing *NSWr*) (Figs 5B, 6, confirming hypothesis H4 of Fig. 2).

Most often heartwood formation has been reported as an age-related process (Wilkes, 1991; Spicer, 2005; Spicer and Holbrook, 2007) associated with the senescence and death of living xylem parenchyma cells (Bamber, 1976; Spicer, 2005). In trees, age is tightly correlated with other size-related variables (Mencuccini *et al.*, 2005). Trees grow in height when they get older, whereas their growth rate (both axial and radial) typically declines during ontogeny (Ryan *et al.*, 1997). Instead, our model simulations corroborated previous indications that sapwood is turned into heartwood once the hydraulic contribution of the innermost sapwood layer (i.e. ring) to the total plant conductance becomes negligible (i.e. sap flow rate has been reported to approximate zero at the sapwood/heartwood transition: Gebauer *et al.*, 2008; Beauchamp *et al.*, 2013). Notably, although hydraulically determined, the model predicted the transition of sapwood into heartwood to occur at a given cambial age all along the stem axis, in agreement with previous reports (Sellin, 1994). Furthermore, we reported that *NSWr* scaled proportionally with *H* and inversely proportionally with *ΔH*, as tree age would also do, thus suggesting that the effect of age on *NSWr* could be indirect and not causal.

In the hydraulic model, we set a threshold of a minimum 0.3% of marginal increase in total plant conductance for maintaining the hydraulic functionality of the innermost sapwood ring, and

thus for setting the transition into heartwood. Accordingly, the model captured the overall scaling of the number of sapwood rings (*NSWr*) with *H* and Δ*H* emerging from our large dataset (cf. Fig. 5A and Supplementary Fig. S3B).

Factors other than *H* and Δ*H* can also affect the radial variation of K_{RING} with *RN*, and therefore the predicted *NSWr*, namely the widening exponent (*b*) (Fig. 8A) and the radial conductivity (k_{RAD}) (Fig. 8C).

Indeed, intra- and interspecific differences in the range of *b*=0.1 to >0.3 can be appreciated across different studies (Petit *et al.*, 2010; Prendin *et al.*, 2018b; Williams *et al.*, 2019), with fast growing trees often showing higher values of *b*. Therefore, it seems very likely that our global dataset accounts for species with different hydraulic architectures and with different scaling parameters of axial conduit widening (*a* and *b* of Equation 1).

We accounted for the entire observed range of *b* across trees (but maintained along the different annual xylem rings) by running simulations implementing two scenarios with *b*=0.15 and *b*=0.3, as well as with *b*=0. Notably, the model predicted the variation in *NSWr* with *H* in a similar manner to the statistical fit for trees (mostly conifers) with reduced Δ*H* (Fig. 5A) when the scaling exponent of axial conduit widening was appropriate for mature conifer trees (*b*=0.15) (Fig. 3; Supplementary Table 3A). At the other extreme, the model only slightly overestimated *NSWr* for fast growing trees (mostly angiosperms) when *b*=0.3 was implemented in the simulations. Consistently, angiosperm trees have often been reported to be characterized by a higher *b* [e.g. in the analysed *F. sylvatica* tree *b*=0.22; in *Eucalyptus regnans* F. Muell. *b*>0.25 (Petit *et al.*, 2010; Williams *et al.*, 2019)].

Furthermore, the radial conductivity (k_{RAD}) possibly also represents a source of variation for the radial variation of K_{RING} with *RN*, and therefore *NSWr* and may also differ between angiosperms and conifers.

In the base case of our simulations, k_{RAD} was consistent with the very few estimate found in the literature for conifer trees (Domec *et al.*, 2006; Barnard *et al.*, 2013) and was kept constant along the given ring. Model simulations run with varying k_{RAD} revealed that very low k_{RAD} decreases the total tree hydraulic conductance, whereas k_{RAD} larger than a certain threshold no longer affects the total tree hydraulic conductance (Fig. 8C). No information about the possible magnitude of variation in k_{RAD} which may occur across conifer and angiosperm trees is available in the literature. However, it seems very likely that the actual ring-to-ring conductance depends on the tree ring anatomy, and therefore would be species specific and dependent on the position within the tree. For instance, in conifers, intertracheary bordered pits are commonly displayed on radial walls in earlywood tracheids and on tangential walls in latewood tracheids (Carlquist, 2017), probably suggesting that earlywood and latewood are not well integrated hydraulically. In broadleaved trees, clusters of few large vessels embedded in a matrix of thick-walled fibres confer hydraulic compartmentalization even at the scale of tree ring sectors (Ellmore *et al.*, 2006).

Notably, the scaling of *NSWr* with *H* and Δ*H* was found to be independent of ring width (Fig. 7B), and thus of the absolute ring conductivity (not conductance).

Our results suggest that the relative allocation to new xylem biomass production and metabolic maintenance of sapwood rings (i.e. the living cells therein) would change according to the contribution of inner rings to the total hydraulic conductance, which was shown to be independently affected by *H* and Δ*H*. This supports the hypothesis that trees maintain the innermost sapwood ring until the carbon costs associated with the maintenance of its living cells are lower than those for the production of new vascular elements equally contributing to the total hydraulic conductance. This would explain why *NSWr* decreases with Δ*H*, but also would allow a more thorough understanding of the physiological consequences of the well-known trends of progressively decreasing height and diameter growth rate with increasing tree size (Mencuccini *et al.*, 2005): both increasing *H* and decreasing Δ*H* positively affect the contribution of inner rings to the total conductance (H2 of Fig. 1 and H4 of Fig. 2), allowing the tree to reduce the overall carbon costs associated with K_{LEAF} by exploiting the hydraulic conductance of more sapwood rings while reducing the allocation to new xylem biomass.

Taken together, our observations and model predictions open up a future new research avenue on the functional effects of allocation to new xylem biomass (i.e. growth) and maintenance respiration of hydraulically functional sapwood, possibly shedding novel important light on the tight relationship between the tree carbon and water economies (Petit *et al.*, 2016, 2018), which could play a key role in the process of acclimation to different and changing environmental conditions.

Supplementary data

The following supplementary data are available at *JXB* online.

Table S1. Results of the optimal Bayesian models predicting the $\log_{10}DCA$ and $\log_{10}H$ effects on the hydraulic diameter in *P. abies* and *F. sylvatica*.

Table S2. Results of the optimal Bayesian models predicting the effects of $\log_{10}DCA$ and *H* classes on the hydraulic diameter in *P. abies* and *F. sylvatica*.

Table S3. Results of the optimal linear mixed-effect models predicting the effects of $\log_{10}H$ and Δ*H* classes on the number of sapwood rings and of $\log_{10}\Delta H$ and Division (Conifers/Angiosperms) on the mean width of sapwood rings.

Fig. S1. Schematic representation of the hydraulic model and comparison between model configurations differing in stem elongation rate (Δ*H*).

Fig. S2. Model prediction of the decline in ring conductance (K_{RING}) and increase in cumulative conductance (K_{CUM}) with the ring number (*RN*) counted from the stem periphery inwards.

Fig. S3. Relationship between *NSWr* and tree height (*H*) assessed for different classes of annual stem height increment (ΔH=cm year^{-1}).

Fig. S4. Relationship between *NSWr* and ΔH assessed for different *H* classes.

Acknowledgements

We warmly thank Davide Giurini and Alessandro Farinati for their contribution in field sampling, sample preparation, and measurements.

Author contributions

GP: conceptual design, with the help of MM and TH; GP and ALP: conducting the anatomical measurements and relative data analyses; TH: developing the numerical model, with the help of GP and MM; MC: providing the biometric parameters of trees from field sampling in the Italian Alps; GP: writing the manuscript with essential contributions by MM and TH. All co-authors contributed by discussing and reviewing the drafts and final version.

Conflict of interest

None declared.

Funding

GP was supported by the University of Padova (DOR2111477/21). ALP was supported by the 2017 BIRD Project of TeSAF Department University of Padova.

Data availability

The data that support the findings of this study are openly available at the Dryad Digital Repository (https://doi.org/10.5061/dryad.pg4f4qrv9; Petit *et al.*, 2023).

References

Anfodillo T, Deslauriers A, Menardi R, Tedoldi L, Petit G, Rossi S. 2012. Widening of xylem conduits in a conifer tree depends on the longer time of cell expansion downwards along the stem. Journal of Experimental Botany **63**, 837–845.

Anfodillo T, Petit G, Crivellaro A. 2013. Axial conduit widening in woody species: a still neglected anatomical pattern. IAWA Journal **34**, 352–364.

Aniol RW. 1987. A new device for computer assisted measurement of tree-ring widths. Dendrochronologia **5**, 135–141.

Bamber RK. 1976. Heartwood, its function and formation. Wood Science and Technology **10**, 1–8.

Barnard DM, Lachenbruch B, McCulloh KA, Kitin P, Meinzer FC. 2013. Do ray cells provide a pathway for radial water movement in the stems of conifer trees? American Journal of Botany **100**, 322–331.

Beauchamp K, Mencuccini M, Perks M, Gardiner B. 2013. The regulation of sapwood area, water transport and heartwood formation in Sitka spruce. Plant Ecology and Diversity **6**, 45–56.

Becker P, Gribben RJ, Lim CM. 2000. Tapered conduits can buffer hydraulic conductance from path-length effects. Tree Physiology **20**, 965–967.

Bürkner P-C. 2017. brms: an R package for Bayesian multilevel models using Stan. Journal of Statistical Software **80**, 1–28.

Carlquist S. 2017. Conifer tracheids resolve conflicting structural requirements. Journal of the Botanical Research Institute of Texas **11**, 123–141.

Carrer M, Von Arx G, Castagneri D, Petit G. 2015. Distilling allometric and environmental information from time series of conduit size: the standardization issue and its relationship to tree hydraulic architecture. Tree Physiology **35**, 27–33.

Domec JC, Meinzer FC, Gartner BL, Woodruff D. 2006. Transpiration-induced axial and radial tension gradients in trunks of Douglas-fir trees. Tree Physiology **26**, 275–284.

Duncan RP. 1989. An evaluation of errors in tree age estimates based on increment cores in Kahikatea (*Dacrycarpus dacrydioides*). New Zealand Natural Sciences **16**, 31–37.

Echeverría A, Anfodillo T, Soriano D, Rosell JA, Olson ME. 2019. Constant theoretical conductance via changes in vessel diameter and number with height growth in *Moringa oleifera*. Journal of Experimental Botany **70**, 5765–5772.

Ellmore GS, Zanne AE, Orians CM. 2006. Comparative sectoriality in temperate hardwoods: hydraulics and xylem anatomy. Botanical Journal of the Linnean Society **150**, 61–71.

Falster DS, Duursma RA, Ishihara MI, *et al*. 2015. BAAD: a biomass and allometry database for woody plants. Ecology **96**, 1445.

Fiora A, Cescatti A. 2008. Vertical foliage distribution determines the radial pattern of sap flux density in *Picea abies*. Tree Physiology **28**, 1317–1323.

Gartner BL, Meinzer FC. 2005. Structure–function relationships in sapwood water transport and storage. In: Holbrook NM, Zwieniecki MA, eds. Vascular transport in plants. Amsterdam: Elsevier Academic Press, 307–331.

Gebauer T, Horna V, Leuschner C. 2008. Variability in radial sap flux density patterns and sapwood area among seven co-occurring temperate broad-leaved tree species. Tree Physiology **28**, 1821–1830.

Givnish TJ, Wong SC, Stuart-Williams H, Holloway-Phillips M, Farquhar GD. 2014. Determinants of maximum tree height in *Eucalyptus* species along a rainfall gradient in Victoria, Australia. Ecology **95**, 2991–3007.

James SA, Clearwater MJ, Meinzer FC, Goldstein G. 2002. Heat dissipation sensors of variable length for the measurement of sap flow in trees with deep sapwood. Tree Physiology **22**, 277–283.

Jiménez MS, Nadezhdina N, Čermák J, Morales D. 2000. Radial variation in sap flow in five laurel forest tree species in Tenerife, Canary Islands. Tree Physiology **20**, 1149–1156.

Kiorapostolou N, Petit G. 2019. Similarities and differences in the balances between leaf, xylem and phloem structures in *Fraxinus ornus* along an environmental gradient. Tree Physiology **39**, 234–242.

Kiorapostolou N, Camarero JJ, Carrer M, Sterck F, Brigita B, Sangüesa-Barreda G, Petit G. 2020. Scots pine trees react to drought by increasing xylem and phloem conductivities. Tree Physiology **40**, 774–781.

Koçillari L, Olson ME, Suweis S, *et al*. 2021. The widened pipe model of plant hydraulic evolution. Proceedings of the National Academy of Sciences, USA **118**, e2100314118.

Kolb KJ, Sperry JS. 1999. Differences in drought adaptation between subspecies of sagebrush (*Artemisia tridentata*). Ecology **80**, 2373–2384.

Maton C, Gartner BL. 2005. Do gymnosperm needles pull water through the xylem produced in the same year as the needle? American Journal of Botany **92**, 123–131.

Mencuccini M, Martinez-Vilalta J, Vanderklein D, Hamid HA, Korakaki E, Lee S, Michiels B. 2005. Size-mediated ageing reduces vigour in trees. Ecology Letters **8**, 1183–1190.

Mencuccini M, Hölttä T, Petit G, Magnani F. 2007. Sanio's laws revisited. Size-dependent changes in the xylem architecture of trees. Ecology Letters **10**, 1084–1093.

Olson ME, Anfodillo T, Gleason SM, McCulloh KA. 2021. Tip-to-base xylem conduit widening as an adaptation: causes, consequences, and empirical priorities. New Phytologist **229**, 1877–1893.

Olson ME, Anfodillo T, Rosell JA, Petit G, Crivellaro A, Isnard S, León-Gómez C, Alvarado-Cárdenas LO, Castorena M. 2014. Universal hydraulics of the flowering plants: vessel diameter scales with stem length across angiosperm lineages, habits and climates. Ecology Letters **17**, 988–997.

Olson ME, Soriano D, Rosell JA, *et al*. 2018. Plant height and hydraulic vulnerability to drought and cold. Proceedings of the National Academy of Sciences, USA **115**, 7551–7556.

Petit G, Anfodillo T. 2009. Plant physiology in theory and practice: an analysis of the WBE model for vascular plants. Journal of Theoretical Biology **259**, 1–4.

Petit G, Anfodillo T, Carraro V, Grani F, Carrer M. 2011. Hydraulic constraints limit height growth in trees at high altitude. New Phytologist **189**, 241–252.

Petit G, Mencuccini M, Carrer M, Prendin AL, Hölttä T. 2023. Data from: Axial conduit widening, tree height, and height growth rate set the hydraulic transition of sapwood into heartwood. Dryad Digital Depository https://doi.org/10.5061/dryad.pg4f4qrv9

Petit G, Pfautsch S, Anfodillo T, Adams MA. 2010. The challenge of tree height in *Eucalyptus regnans*: when xylem tapering overcomes hydraulic resistance. New Phytologist **187**, 1146–1153.

Petit G, Savi T, Consolini M, Anfodillo T, Nardini A. 2016. Interplay of growth rate and xylem plasticity for optimal coordination of carbon and hydraulic economies in *Fraxinus ornus* trees. Tree Physiology **36**, 1310–1319.

Petit G, von Arx G, Kiorapostolou N, *et al*. 2018. Tree differences in primary and secondary growth drive convergent scaling in leaf area to sapwood area across Europe. New Phytologist **218**, 1383–1392.

Phillips N, Oren R, Zimmermann R. 1996. Radial patterns of xylem sap flow in non-, diffuse- and ring-porous tree species. Plant, Cell & Environment **19**, 983–990.

Pothier D, Margolis HA, Waring RH. 1989. Patterns of change of saturated sapwood permeability and sapwood conductance with stand development. Canadian Journal of Forest Research **19**, 432–439.

Prendin AL, Mayr S, Beikircher B, Von Arx G, Petit G. 2018a. Xylem anatomical adjustments prioritize hydraulic efficiency over safety as Norway spruce trees grow taller. Tree Physiology **38**, 1088–1097.

Prendin AL, Petit G, Fonti P, Rixen C, Dawes MA, von Arx G. 2018b. Axial xylem architecture of *Larix decidua* exposed to CO_2 enrichment and soil warming at the tree line. Functional Ecology **32**, 273–287.

Quiñonez-Piñón MR, Valeo C. 2018. Assessing the translucence and color-change methods for estimating sapwood depth in three boreal species. Forests **9**, 686.

R Development Core Team. 2022. R: a language and environment for statistical computing. Vienna, Austria: R Foundation for Statistical Computing.

Ryan MG, Binkley D, Fownes JH. 1997. Age-related decline in forest productivity: pattern and process. Advances in Ecological Research **27**, 213–262.

Sanio K. 1872. Uber die grosse der holzzellen bei der gemeinen der kiefer (*Pinus sylvestris*). Jahrbucher für Wissenschaftliche Botanik **8**, 401–420.

Schulte PJ. 2012. Vertical and radial profiles in tracheid characteristics along the trunk of Douglas-fir trees with implications for water transport. Trees **26**, 421–433.

Sellin A. 1994. Sapwood–heartwood proportion related to tree diameter, age, and growth rate in *Picea abies*. Canadian Journal of Forest Research **24**, 1022–1028.

Shinozaki K, Yoda K, Hozumi K, Kira T. 1964. A quantitative analysis of plant form—the pipe model theory I. Basic analyses. Japanese Journal of Ecology **14**, 94–105.

Sousa VB, Cardoso S, Pereira H. 2013. Ring width variation and heartwood development in *Quercus faginea*. Wood and Fiber Science **45**, 405–414.

Spicer R. 2005. Senescence in secondary xylem: heartwood formation as an active developmental program. In: Holbrook NM, Zwieniecki MA, eds. Vascular transport in plants. Amsterdam: Elsevier Academic Press, 457–475.

Spicer R, Gartner BL. 2001. The effects of cambial age and position within the stem on specific conductivity in Douglas-fir (*Pseudotsuga menziesii*) sapwood. Trees **15**, 222–229.

Spicer R, Holbrook NM. 2007. Effects of carbon dioxide and oxygen on sapwood respiration in five temperate tree species. Journal of Experimental Botany **58**, 1313–1320.

Stokes MA, Smiley TL. 1968. Introduction to tree-ring dating. Chicago: University of Chicago Press.

Tyree MT, Ewers FW. 1991. The hydraulic architecture of trees and other woody plants. New Phytologist **119**, 345–360.

von Arx G, Carrer M. 2014. ROXAS—a new tool to build centuries-long tracheid–lumen chronologies in conifers. Dendrochronologia **32**, 290–293.

Wason JW, Brodersen CR, Huggett BA. 2019. The functional implications of tracheary connections across growth rings in four northern hardwood trees. Annals of Botany **124**, 297–306.

Weitz JS, Ogle K, Horn HS. 2006. Ontogenetically stable hydraulic design in woody plants. Functional Ecology **20**, 191–199.

West GB, Brown JH, Enquist BJ. 1999. A general model for the structure and allometry of plant vascular systems. Nature **400**, 664–667.

Wilkes J. 1991. Heartwood development and its relationship to growth in *Pinus radiata*. Wood Science and Technology **25**, 85–90.

Williams CB, Anfodillo T, Crivellaro A, Lazzarin M, Dawson TE, Koch GW. 2019. Axial variation of xylem conduits in the Earth's tallest trees. Trees **33**, 1299–1311.

Zhao H, Yang S, Guo X, Peng C, Gu X, Deng C, Chen L. 2018. Anatomical explanations for acute depressions in radial pattern of axial sap flow in two diffuse-porous mangrove species: implications for water use. Tree Physiology **38**, 276–286.